Rare Metal Materials and Engineering
Volume 47, Issue 8, August 2018
Online English edition of the Chinese language journal

Available online at www.sciencedirect.com
ScienceDirect

Cite this article as: Rare Metal Materials and Engineering, 2018, 47(8): 2322-2327.

ARTICLE

Fabrication, Characterization of Ultra-low-density Bulk Nanoporous Gold with Uniform Structure and Volume Shrinkage Control During Drying

Liu Chaoqing, Lian Lixian, Liu Ying, Li Qin

Sichuan University, Chengdu 610065, China

Abstract: Ultra-low-density bulk nanoporous gold (NPG) is required in inertial confined fusion (ICF) experiments. Existing bulk NPG has some limitations in ICF application due to non-uniformity structure or residues of C originated from organic template. Here, combined with dealloying, NPG with submicron cavities and nanopores was prepared by nano-SiO_2 templates. However, the smaller templates bring greater challenges for the volume shrinkage control during drying as gold content on each shell is extremely low for ultra-low density. Therefore, the influence of drying methods on volume shrinkage was investigated. The results show that volume shrinkage is up to 86.41% during conventional drying, but it is controlled below 4% by supercritical CO_2 drying. Finally, NPG with ultra-low-density of 0.35 g/cm^3 was fabricated. Compared to NPG prepared by micro templates, the NPG with 500 nm spherical cavities and 2~70 nm nanopores reduces the size difference between large cavities and nanopores and significantly improves the uniformity of its structure.

Key words: nanoporous gold; ultra-low-density; template-dealloying; supercritical drying

Porous metal materials are widely applied in the field of heat exchange, catalysis, battery electrode, filtration and separation as they combine properties of metals with porous materials, such as good thermal and electrical conductivity, catalytic activity, high specific surface areas and good permeability[1-7]. Among these porous metal materials, nanoporous gold (NPG), which holds high radiation opacity (high *Z*) and porous architecture, can reduce the energy loss of X-ray and obtain the high radiation temperature[8,9]. Therefore, bulk NPG is attractive material in high energy density experiments, especially in ICF used as hohlraum walls[10-14].

There are numerous synthetic strategies for fabricating porous gold, including dealloying, electrochemical method, templating, self-assembly, powder metallurgy, and so on[15-20]. Among these methods, the technique of combining templating with dealloying is more conducive to obtaining bulk NPG that meets the requirements in ICF[10,12,14]. Nyce et al. successfully prepared ultra-low-density porous gold using polystyrene (PS) microspheres as templates with the template-dealloying method[10,11]. The results indicate that the porous gold holds 10 and 1 μm cavities and abundant C elements residues after pyrolysis of PS templates. However, the thickness of cylindrical hohlraum wall is usually a few microns and the existence of large cavities in several microns makes the original porous structure easy to be damaged during the subsequent processing. In addition, smaller spherical cavities can reduce the X-ray energy loss and improve radiation temperature more effectively[21,22].

Decreasing the size of sacrificial template can obtain smaller cavities and more uniform structures. The NPG prepared by template-dealloying is composed of hollow shells with porous structure. In order to obtain an ultra-low density, the gold content of each unit area on each shell should be extremely reduced with smaller templates so that the hollow shell will be more fragile and easily deformed. Therefore, smaller templates bring greater challenges for volume

Received date: August 19, 2017
Foundation item: Science and Technology Support Project of Sichuan Province (2014GZ0137, 2016GZ0225)
Corresponding author: Lian Lixian, Ph. D., Professor, School of Materials Science & Engineering, Sichuan University, Chengdu 610065, P. R. China, Tel: 0086-28-85405332, E-mail: scu_lianyi@126.com

shrinkage control during drying process. In our earlier work, the porous structure of NPG was damaged seriously and bulk density increased dramatically in conventional drying process.

To solve these problems, SiO_2 spheres with diameter of about 500 nm were introduced as templates and bulk NPG was dried by supercritical CO_2 drying in the present study. The original structure of the porous gold was retained and volume shrinkage was controlled below 4% via supercritical drying. Ultra-low-density bulk NPG with submicron cavities and nanopores was fabricated.

1 Experiment

SiO_2 spheres served as templates with diameters of 500 nm were prepared by Stöber method. For a density of about 0.3 g/cm^3, the mass ratio of gold, silver and 500 nm SiO_2 should be about 3:4:4 by calculation. Ag and Au were deposited on SiO_2 surface in sequence through electroless plating. The SiO_2 spheres were sensitized in $SnCl_2$ solution (15 g/L) and activated in $AgNO_3$ solution (5 g/L). The mixture solution of glu cose (8 g/L) and potassium sodium tartrate (15 g/L) boiled and cooled was used as a reducing agent. The reducing agent solu tion was added into 50 mL mixture solutions of activated SiO_2 and silver plating solution ($AgNO_3$: 10 g/L, NaOH: 5 g/L) dropwise accompanied by magnetic stirring. The load of SiO_2 was 6 g/L. SiO_2@Ag composite particles were obtained after washing, centrifugating and drying at 50 °C. The SiO_2@Ag suspension was added into 150 mL gold plating solution ($HAuCl_4 \cdot 4H_2O$: 3 g/L, Na_2CO_3: 17.5 g/L). Methanol and polyvinylpyrrolidone (PVP, K30) were incorporated into the solution as a reducing agent and a stabilizing agent, respectively.

Cylindrical SiO_2@Ag@Au bulk was formed by the filter-casting method with teflon tube (Φ5 mm) as a forming mould and plaster of paris block as a water-absorbing agent. The SiO_2@Ag@Au bulk precursor after drying and demoulding were sintered at 500 °C for 1 h under Ar atmosphere. SiO_2 was etched by hydrofluoric acid (HF) and Ag component was dealloyed by nitric acid (HNO_3). Fig.1 shows the schematic illustration of the corrosion process. Part of Ag was firstly corroded at the early stage by 1.5 mol/L HNO_3, and then HF was added to etch SiO_2. The concentration of HNO_3 was increased to 12 mol/L by 0.6 mol/L every 24 h. After dealloying, residual HNO_3 was removed by washing several times with deionized water and ethanol in sequence before drying. NPG was dried by conventional drying or supercritical CO_2 drying. The conventional drying was carried out under normal temperature and pressure. In the supercritical CO_2 drying process, the working temperature was 40 °C and the internal pressure inside was set at 10 MPa.

Morphology and elemental composition of the samples were characterized by a field emission scanning electron microscope (FESEM, FEI INSPECT-F50) equipped with an X-ray energy spectrometer (EDS). The size of Ag particles on

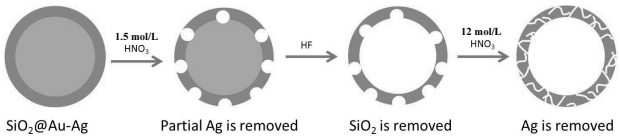

Fig.1 Schematic illustration of corrosion process

SiO_2 surfaces was counted by Image-Pro Plus from the SEM images. The phase evolution of the samples of electroless plating and corrosion was identified by an X-ray diffrac-tometer (XRD, DX-2700) with Cu Kα radiation operating at 40 kV and 30 mA. The microstructure of the porous gold ligaments was characterized by a transmission electron microscope (TEM, JEOL JEM-2100F). Nitrogen adsorption measurements were conducted using a micromeritics ASAP 2460 analyzer. The bulk NPG obtained in the present paper was a regular cylinder, so the volume and mass of the sample could be measured and the density could be calculated directly.

2 Results and Discussion

2.1 Microstructure evolution of bulk nanoporous gold

Fig.2 is the SEM images and the EDS results of samples at different stages of fabrication. Fig.2a, 2c, 2e, 2g and 2i show the morphology evolution and Fig.2b, 2d, 2f, 2h and 2j exhibit composition change. Fig.2a shows that Ag layer is composed of independent island Ag nanoparticles. Fig.2b confirms that Ag is deposited on SiO_2 surface. Compared to Fig.2a, the metal layer becomes more compact and the final surface morphology of SiO_2@Ag@Au particles is dependent on the coating structure of silver layer as shown in Fig.2c. It can be identified that Au particles are deposited on SiO_2@Ag particles and the atomic percentage of Ag and Au is about 7:3 from EDS results in Fig.2d. The crystal structures of Au and Ag are almost identical and the interfacial energy between Au and Ag is very small. Therefore, Au atoms could easily nucleate and grow on Ag particles surface to encapsulate Ag particles first and then extend to the gap. As can be seen from Fig.2c, the diameter of SiO_2@Ag@Au particles is about 610 nm. The thickness of double metal layer is about 55 nm.

SiO_2@Ag@Au particles were formed into a cylinder, and the cylinder was calcined to obtain Ag-Au alloy for the following dealloying. Fig.2e is the SEM image of SiO_2@Ag@Au bulk after calcining at 500 °C for 1 h under Ar atmosphere. Compared to Fig.2c, the metal layer becomes smoother and the initial morphology of SiO_2@Ag@Au particles changes as shown in Fig.2e. As can be seen from Fig.2e, the diameter of SiO_2@Ag-Au particles is about 600 nm, which is slightly smaller than that of SiO_2@Ag@Au particles. EDS analysis in Fig.2f also confirms that the atomic ratio of Ag to Au is about 7:3. Due to the reduction of oxygen content detected by EDS, the contents of Ag and Au

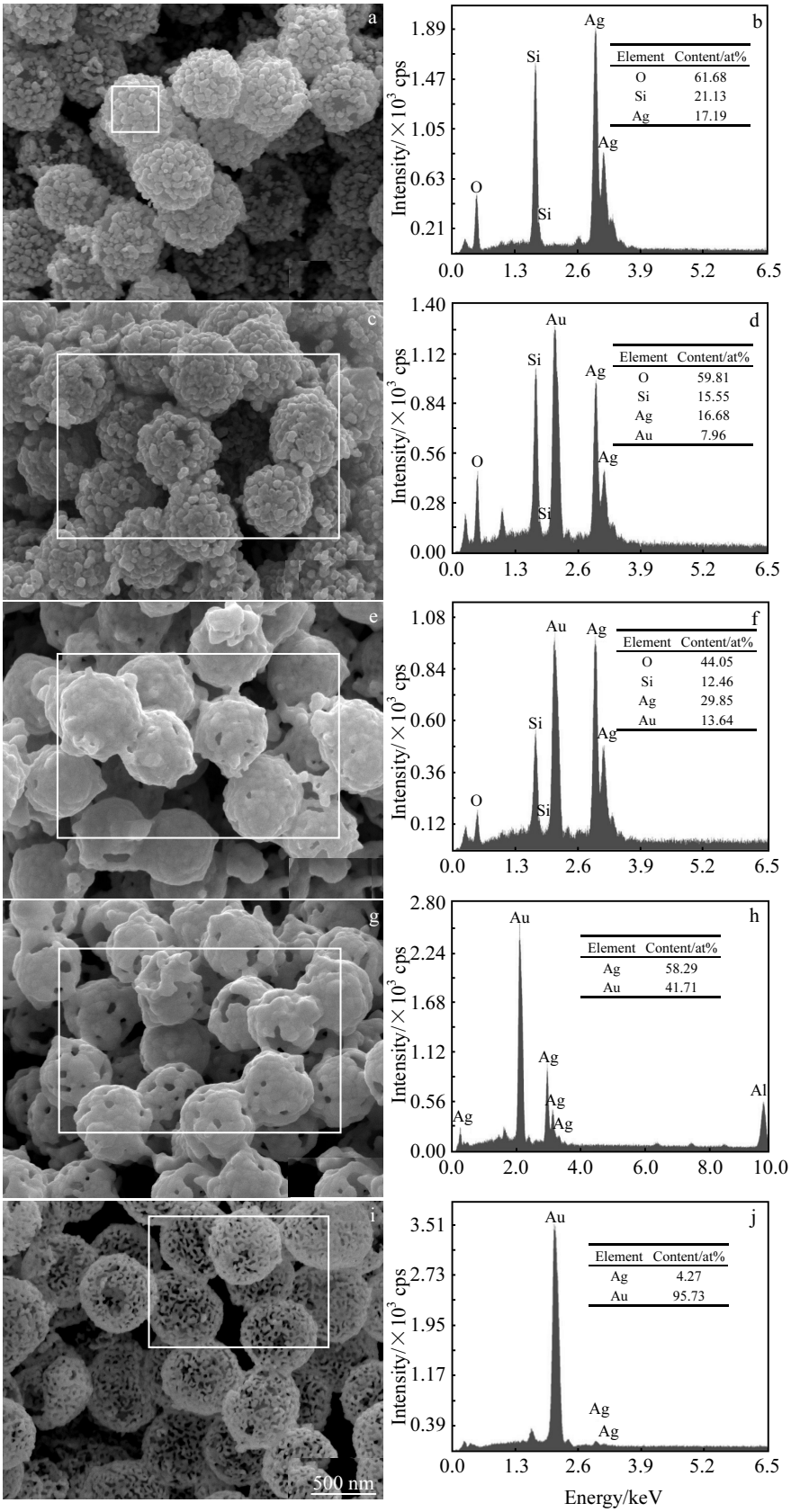

Fig.2 SEM images (a, c, e, g, i) and EDS results (b, d, f, h, j) of samples at different stages of fabrication: (a, b) SiO_2@Ag particles, (c, d) SiO_2@Ag@Au particles, (e, f) SiO_2@Ag@Au bulk after calcining (SiO_2@Ag-Au bulk), (g, h): SiO_2@Ag-Au bulk after removing part of Ag and SiO_2 removed, and (i, j) bulk NPG by supercritical drying

increase by comparison with the EDS results in Fig.2d, as shown in Fig.2f. Nanoparticle holds a high specific surface area and a high activity. Therefore, a process similar to powder sintering easily occurs between the intimately contacted particles of double metal layer during short-time heat treatment. Sintering necks initially form between the adjacent Ag (Au) particles and the metal layers become smooth with the growth of sintering necks in the heat preservation process. Fig.2e also indicates the sintering necks form between some composite particles, which is favorable for avoiding the collapse of bulk during the subsequent corrosion process.

SiO_2 spheres were soluble templates and could be removed by HF. Ag, as the less noble constituent, could be selectively dissolved by HNO_3 from Ag-Au alloy. A great amount of gas would be produced in both processes of removal of SiO_2 and dissolution of Ag, which will lead to cracking of the bulk if the concentration of HNO_3 (HF) is too high. Therefore, the concentration should be well controlled and increased from low to high gradually. SiO_2 and Ag were removed alternately in the process of corrosion, as shown in Fig.1. A small amount of Ag elements are dissolved firstly and small pores form on the alloy layer, which is conductive to the entry of hydrofluoric acid and the discharge of gas. Fig.2g shows that self-supporting hollow shells with small pores are obtained. The EDS result in Fig.2h shows SiO_2 templates are completely removed and the atomic percentage of Ag decreases by comparison with Au. With further increase of the concentration of HNO_3, the pore structure of the shells gradually transforms into ligament structure as shown in Fig.2i. In the process of dealloying, surface Ag atoms are dissolved firstly, and the Au atoms with no coordination aggregate into clusters on the surface of the alloy. Partial surface is passivated by the pure Au clusters. Ag atoms in the alloy region exposed to nitric acid are continuously dissolved and the newly released gold atoms migrate to the original gold clusters. Therefore, pits or pores form. Due to the thin alloy layer, the etch spread laterally. New Au clusters and new pores form with the further dissolving of Ag atoms and monolayer continuous ligament formation is evolved[23,24]. The EDS result in Fig.2j indicates only a very small amount of silver remains. The bulk porous gold composed of Au hollow spherical shells with nanoporous structures was successfully prepared in solution when the corrosion process was done.

XRD patterns in Fig.3 show the phase evolution in the fabrication process of bulk NPG. The SiO_2 prepared by Stöber method is amorphous. Compared to the SiO_2, Ag diffraction peaks were clearly observed in SiO_2@Ag particles, indicating that Ag was successfully coated onto SiO_2. And this is consistent with the EDS result in Fig.2b. There is no obvious difference could be seen between SiO_2@Ag particles and SiO_2@Ag@Au particles due to the similar lattice constants between Au and Ag. Therefore, the existence of gold could not

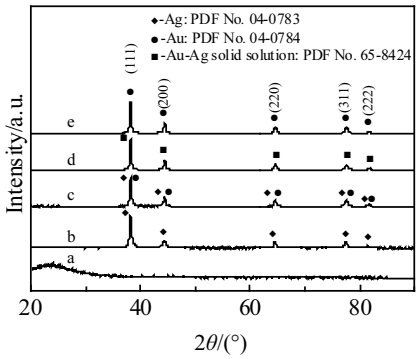

Fig.3 XRD patterns of samples at different stages of fabrication: (a) SiO_2, (b) SiO_2@Ag particles, (c) SiO_2@Ag@Au particles, (d) SiO_2@Ag-Au bulk, and (e) bulk NPG

be determined only by the XRD result. Nevertheless, the information of EDS result in Fig.2d could shed some light on the existence of gold. High diffusion rate of Au and Ag atoms at medium temperature, similar crystal structure, and very close lattice constants, all these made the alloying reaction take place readily. It could be inferred that $Ag_{0.7}Au_{0.3}$ solid solution was obtained after calcined from the XRD pattern of SiO_2@Ag-Au bulk combined with the EDS result in Fig.2f. The atomic percentage of Ag is below 5% as shown in the EDS result in Fig.2j. Therefore, it further proves that the df fraction peaks in the XRD pattern of bulk NPG only belong to Au.

2.2 Volume shrinkage control during drying

The drying of as-prepared bulk NPG was challenging. Table 1 shows volume shrinkage rate, relative density and porosity of bulk NPG after treated by conventional drying and supercritical CO_2 drying. As can be seen from Table 1, the volume shrinkage rate of conventionally dried NPG is about 23 times higher than that of supercritical dried NPG. The bulk density increases sharply and porosity decreases dramatically during conventional drying process. The design density could be basically retained with supercritical drying and porosity was as high as 98.19%.

Fig.4a and 4b are SEM images of NPG treated by conventional drying and supercritical drying. Fig.4a shows NPG hollow shells are deformed seriously. Therefore, the increasing density is mainly due to the damage of the porous microstructure. Compared to Fig.4a, the hollow shells and ligament structure of the porous gold are retained much better

Table 1 Effect of drying method on shrinkage rate, relative density and porosity of bulk NPG

Drying method	Volume shrinkage rate/%	Relative density/g·cm^{-3}	Porosity/ %
Conventional drying	86.41	2.98	84.58
Supercritical drying	3.64	0.35	98.19

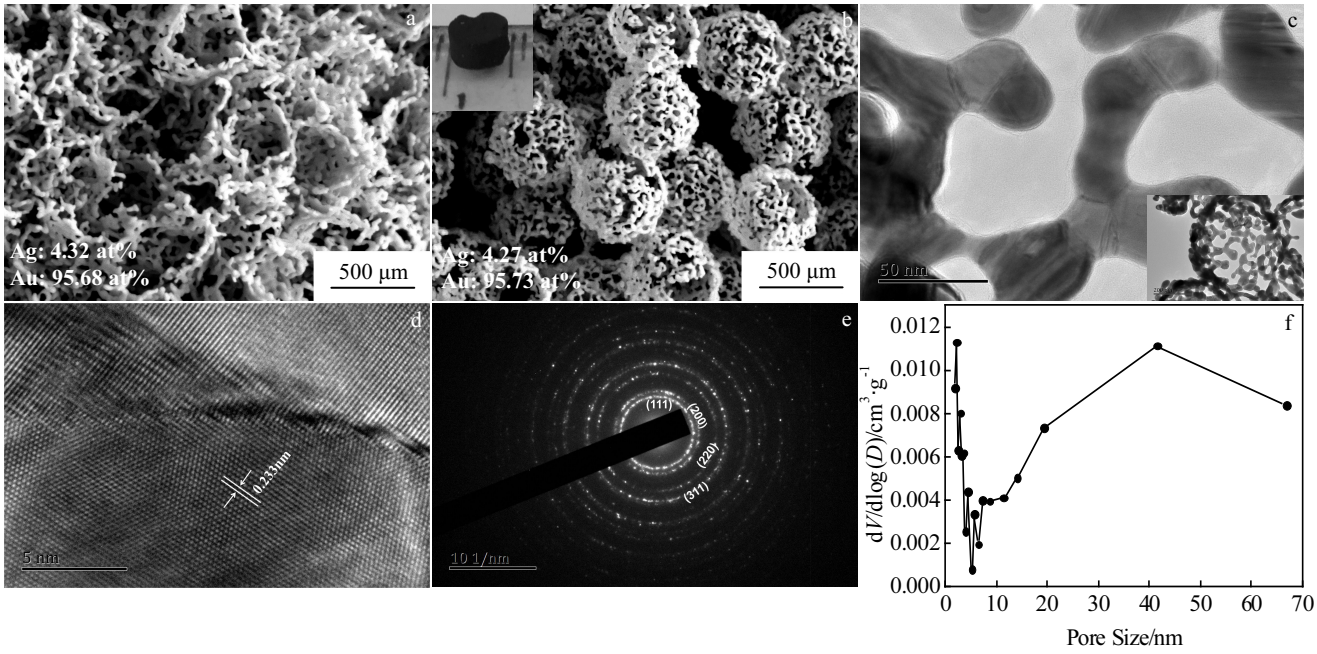

Fig.4 SEM images of NPG by conventional drying (a) and supercritical CO_2 drying (the inset is digital figure) (b); (c) TEM image of NPG ligaments (the inset is TEM image of NPG shell); (d) HRTEM image of Au grain of ligament; (e) SAED pattern of NPG; (f) pore size distribution of NPG

when treated by supercritical drying as shown in Fig.4b. The physical map inserted in Fig.4b shows the as-obtained cylindrical bulk NPG (diameter=4.9 mm, height=2.7~2.8 mm). The porous bulk sample infiltrated by liquid is seen as a capillary porous body before drying. The capillary force is generated with the evaporation of liquid. The porous shell walls on both sides of the capillary are subjected to surface tension. The hollow shells are squeezed and deformed as the pull exceeds the tolerance limit of the spherical shell. The pressure difference was also exerted on the wall of ligaments as capillary liquid existing between ligaments evaporated. The vulnerable ligaments would crack and the shells would be further deformed. The volume shrinkage of bulk NPG was clearly observed and the density increases rapidly. The liquid-vapor phase boundary would disappear and the surface tension is almost zero when the ambient temperature and pressure exceed the critical point of fluid[25, 26]. Therefore, the original structure of NPG could be retained with the supercritical CO_2 drying method. Fig.4b also shows that the diameter of large cavities is about 500 nm.

The inset of Fig.4c is TEM image of a hollow shell and shows the ligaments in the shell are connected together. NPG ligament consists of Au grains with different sizes as shown in Fig.4c. Fig.4d is HRTEM image of Au grain. The interplanar spacing of the grain crystal is measured as 0.233 nm, which is in agreement with the value of Au (111) plane[27]. It further confirms that Au atoms aggregate into nuclei and grow into cubic crystals with the dissolution of Ag atoms. As can be seen from the SAED pattern in Fig.4e, the interconnected ligaments are composed of randomly oriented Au nanocrystals. From inside to outside, the diffraction ring of the SAED pa tern can be indexed as Au (111), (200), (220), and (311) by comparing the XRD results of bulk NPG in Fig.3. The pore size distribution in Fig.4f shows that the size of nanopores is between 2~70 nm.

In summary, in order to reduce the size difference between cavities caused by templates and nanopores caused by dealloying and obtain an ultra-low density at the same time, the gold content of each unit area of the shell should be reduced with smaller templates. And the designed ultra-low density could be retained by controlling the volume shrinkage of bulk NPG with supercritical CO_2 drying.

3 Conclusions

1) Ultra-low-density bulk NPG with density of 0.35 g/cm^3 is prepared by a template-dealloying technique. The NPG exhibits a bimodal porous structure of 500 nm spherical cavities and 2~70 nm nanopores. The ligaments are composed of randomly oriented Au nanocrystals.

2) The drying method dramatically affects not only the morphology and but also the final density of bulk NPG. The original structure of NPG is damaged seriously and the bulk shrinks seriously in conventional drying process due to the existence of capillary force. The hollow shells and ligament structure are preserved perfectly with the supercritical CO_2 drying and the volume shrinkage rate is controlled below ~4%.

3) In addition, the NPG prepared by the template-dealloying method has a good application prospect in gas phase catalytic, electrocatalytic oxidation in fuel cell and purification due to its good mass transport performance facilitated by large cavities and high specific surface area increased by smaller pores.

References

1 Liu S, Feng J K, Bian X F *et al. Nano Energy*[J], 2015, 13: 651
2 Kim D Y, Sung T H, Kim K C. *Energy*[J], 2016, 105: 57
3 Barsuk D, Zadick A, Chatenet M *et al. Materials & Design*[J], 2016, 111: 528
4 Fang X M, Lian L X, Liu Y *et al. Rare Metal Materials and Engineering*[J], 2014, 43(11): 2753 (in Chinese)
5 Tappan B C, Huynh M H, Hiskey M A *et al. Journal of the American Chemical Society*[J], 2006, 128(20): 6589
6 Lefebvre L P, Banhart J, Dunand D C. *Advanced Engineering Materials*[J], 2008, 10(9): 775
7 Tappan B C, Steiner S A, Luther E P. *Angewandte Chemie*[J], 2010, 122(27): 4648
8 Schein J, Jones O, Rosen M *et al. Physical Review Letters*[J], 2007, 98(17): 175 003
9 Rosen M D, Hammer J H. *Physical Review E*[J], 2005, 72(5): 056 403
10 Nyce G W, Hayes J R, Hamza A V *et al. Chemistry of Materials*[J], 2007, 19(3): 344
11 Biener J, Nyce G W, Hodge A M *et al. Advanced Materials*[J], 2008, 20(6): 1211
12 Tan X L, Li K, Bu H *et al. Rare Metal Materials and Engineering*[J], 2015, 44(5): 1273 (in Chinese)
13 Tan X L, Niu G, Li K *et al. Rare Metal Materials and Engineering*[J], 2013, 42(1): 162 (in Chinese)
14 Zhang K B, Tan X L, Zhang J C *et al. RSC Advances*[J], 2014, 4(14): 7196
15 Hodge A M, Hayes J R, Caro J A *et al. Advanced Engineering Materials*[J], 2006, 8(9): 853
16 Chen A Y, Wang J W, Wang Y *et al. Electrochimica Acta*[J], 2015, 153: 552
17 Ikegami M, Hirano Y, Mie Y *et al. Journal of Electroanalytical Chemistry*[J], 2016, 783: 188
18 Cox M E, Dunand D C. *Materials Science and Engineering A*[J], 2011, 528(6): 2401
19 Morag A, Golub T, Becker J *et al. Journal of Colloid and Interface Science*[J], 2016, 472: 84
20 Hao G L, Xu Q P, Wang H *et al. Materials Science and Technology*[J], 2016, 32(15): 1592
21 Gobby P L, Moore J E, Snow R C *et al. Journal of Vacuum Science & Technology A: Vacuum, Surfaces, and Films*[J], 1989, 7(3): 996
22 Reichelt J M A. *Journal of Vacuum Science & Technology A: Vacuum, Surfaces, and Films*[J], 1985, 3(3): 1245
23 Erlebacher J, Aziz M J, Karma A *et al. Nature*[J], 2001, 410(6827): 450
24 Erlebacher J, Sieradzki K. *Scripta Materialia*[J], 2003, 49(10): 991
25 Brown Z K, Fryer P J, Norton I T *et al. Innovative Food Science & Emerging Technologies*[J], 2008, 9(3): 280
26 Gromadzińska E, Rogacki G, Zawadzka A *et al. The Journal of Supercritical Fluids*[J], 2015, 102: 92
27 Kannan P, John S A. *Nanotechnology*[J], 2008, 19(8): 085 602

结构均匀的超低密度纳米多孔金块体制备与表征及其体积收缩的控制

刘朝清，连利仙，刘　颖，李　芹

(四川大学，四川 成都 610065)

摘　要：超低密度纳米多孔金块材是惯性约束聚变（ICF）的目标材料。由于结构的不均匀性和有机模板分解造成的碳元素残留等原因，现有的多孔金在 ICF 应用中有一定的局限性。因此，结合去合金化方法以二氧化硅为模板制备出了具有亚微米级大孔和纳米级小孔的双级孔结构的纳米多孔金块体。然而，模板尺寸的急剧减小使得金含量用量极低而引起样品在干燥过程中严重收缩。因此研究了干燥方式对多孔金体积收缩的影响。结果表明，样品在普通干燥过程中体积收缩高达 86.41%，而采用超临界干燥体积收缩被控制到 4%以下，密度被控制到 0.35 g/cm^3（孔隙率 98.19%）以下。制备的超低密度多孔金明显地缩小了模板留下的大孔（500 nm）和去合金产生的小孔（2~70 nm）之间的尺寸差距，有效地提高了结构的均匀性。

关键词：纳米多孔金；超低密度；模板-去合金化；超临界干燥

作者简介：刘朝清，男，1989 年生，硕士，四川大学材料科学与工程学院，四川 成都 610065，电话：028-85405332，E-mail: liuchaoqing_ariel@126.com